MATURE STAGE EXPERIMENT
Science Description

Experiment/Module: Distribution of Hazardous Winds

Investigator(s): Kelly Ryan (Co-I) and Heather Holbach (Co-I)

Requirements: Categories 2–5

Plain Language Description: Estimating tropical cyclone wind hazards can be difficult and operationally often requires assumptions to be made about surface wind characteristics relative to available flight-level observations. Approximations of surface wind using reconnaissance flight level (700 mb or 850 mb) have been routinely supported by symmetric assumptions, but observational and modeling comparisons suggest departures from this framework, occasionally detecting variations in surface winds both radially (distance from center) and azimuthally (around the storm). Data collected will be used to refine assumptions asymmetrically, estimate the uncertainty in quadrant wind radii, investigate asymmetries in the boundary layer as they relate to wind and wave hazards, and expose potential boundary layer biases in numerical weather and climate models.

Mature Stage Science Objective(s) Addressed:

1) Collect observations targeted at better understanding internal processes contributing to mature hurricane structure and intensity change [*APHEX Goals 1, 3*].
2) Collect observations targeted at better understanding the response of mature hurricanes to their changing environment, including changes in vertical wind shear, moisture and underlying oceanic conditions [*APHEX Goals 1, 3*].

Motivation: Many existing reconnaissance techniques revolve around symmetric coverage regardless of shape or size of a given tropical cyclone (TC) with a strong focus on radial gradients to assess its structure. This continues to drive the many well-documented investigations of TC structure which are crucial in understanding the hazard distribution for a given event based on its symmetric TC "size". However, lack of azimuthal coverage in the inner, and especially the outer core, have limited our understanding of wind field distribution asymmetries and their causes, impacting the capability of existing wave and surge models that are critical to an accurate TC hazard forecast beyond wind hazards alone. As such, NHC regularly reports a radius of maximum winds and significant wind radii values by quadrant (radius of 64-, 50-, and 34-knots winds) which are ingested into the appropriate models for their respective hazard representations.

This quadrant wind information has been crucial for surge and wave models which rely on accurate surface wind and wave characteristics, including the strength and direction of surface winds and significant wave heights. However, the uncertainty in significant wind radii can be quite large (Landsea and Franklin 2013), which is the primary motivation for this observation strategy. Observations collected aim to assess deviations from symmetric mean boundary layer structure to better quantify the potential distribution of hazardous winds.

MATURE STAGE EXPERIMENT
Science Description

Despite the advent of modern computational ocean modeling, wave growth models are heavily limited by the representation of hazardous winds. Even small variations in surface wind speed, direction, and duration can impact significant wave heights and the trapped accumulation of waves related to TC events (Shao et al. 2023, Young 2017, Callaghan et al. 2007, MacAfee and Bowyer 2005, Bowyer et al. 2005, Wright et al. 2001). This has huge implications for surge related hazards, which is sensitive to the vector wind properties. Both static and dynamic fetch calculations for tropical cyclones rely heavily on the distribution of wind speeds along preferential directions. Beyond surface wind observations, wave models are severely limited by the sparsity of wave measurements available and could benefit tremendously from increased coverage in high-wind regimes given evidence of asymmetric wave fields associated with TCs (Esquivel et al. 2015, Hu and Chen 2011, Young 2006).

While better azimuthal coverage is the principal focus, the ability to observe surface wind conditions remains a difficult task especially when measurements reveal conditions departing from conventional assumptions. Mean reduction ratios for flight-level winds from 700 mb or 850 mb to the surface (Franklin et al. 2003) are often used to describe surface wind structure even while real-time measurements indicate uncertainty in this assumption (Uhlhorn et al. 2014, Franklin et al. 2000). A combination of indirect (SFMR, TDR) and direct (dropsondes) reconnaissance surface wind measurements in locations that best describe the individual storm's wind structure can help to quantify uncertainty in these values. Deviations in surface wind estimates among instrumentation tend to occur more often in very strong TCs (Category 3 or higher), and thus are of particular interest regarding surface wind distribution. Furthermore, these data can be used to verify azimuthal structure characteristics seen in large model datasets. Each pattern addresses specific issues related to the uncertainty in reported wind radii values, deviations from conventional symmetric assumptions, and model validation of boundary layer processes affecting the surface wind. These strategies are designed to address azimuthal coverage gaps while maintaining radial coverage necessary for operational hurricane models.

Background: The distribution of surface winds can be difficult to diagnose but is currently best described using the radius of maximum wind and quadrant radii of 34-, 50-, and 64-knot winds provided by NHC. These radii mark the furthest extent of wind speed thresholds in each quadrant and are one way to quantify a TC's size. Nonetheless, much of tropical cyclone science and forecasting techniques rely on axisymmetric assumptions of surface winds while true TCs can be highly asymmetric and exhibit azimuthal variations despite an unchanging overall symmetric size. This is regardless of size definition (Chavas et al. 2016, Knaff et al. 2014, Uhlhorn et al. 2014, Reasor 2000) and algorithms must be implemented to mitigate the lack of azimuthal coverage for both observation- and model-based research. These asymmetries can also heavily influence other TC hazard forecasts, as surface wind and wave information are ingested into wave and surge models both operationally (NHC SLOSH model) and for research purposes (Houghton et al. 2022, Smit et al. 2021).

When studying TC asymmetries, documented research in TC dynamics often takes advantage of axisymmetric assumptions, producing wavenumber decompositions that aid in the understanding of the distribution of hazardous winds in the inner core. This type of polar analysis becomes more complicated in the outer core, where wavenumbers correspond to larger geometric areas as radial distance increases. Furthermore, lack of azimuthal coverage in the inner and outer core have necessitated the use of axisymmetric assumptions to describe hazardous TC conditions. The observation strategies outlined here are designed to improve the representation of the surface wind field distribution based on the individual TC's size and skew from axisymmetry.

By using an approximate distribution shape (Figure 1) estimated by NHC's reported wind radii, an asymmetric flight pattern may be better able to reflect the true wind distribution. Beyond a more precise quantification of hazardous wind distribution, the azimuthal resolution is effectively scaled by radius from the center, allowing for better azimuthal coverage of observations. Figure 1 describes the geometry of estimating the wind distribution of 34-knot winds given asymmetric quadrant wind radii. The properties of the distribution include an estimate of spatial area and a displacement from axisymmetry, including a skew and its orientation. These metrics are calculated using two circles (given quadrant radii) which define major and minor axes of the ellipsoid. The shift in center position of the imaginary circles defines the ellipsoid skew and its azimuthal orientation. This distribution shape could be influenced by both inner core dynamics and environmental gradients, such as convection, motion, and vertical wind shear, and can be applied to large datasets to identify processes and biases in TC boundary layer structure representation. Zhang et al. 2011 describes the most in-depth analysis of dynamic and thermodynamic boundary layer characteristics using GPS dropsonde data, but axisymmetric assumptions were required to obtain radial wind distribution information. Relaxing these assumptions by increasing azimuthal coverage may shed light on asymmetric boundary layer processes that remain difficult to observe such as height of maximum winds and inflow characteristics.

MATURE STAGE EXPERIMENT
Science Description

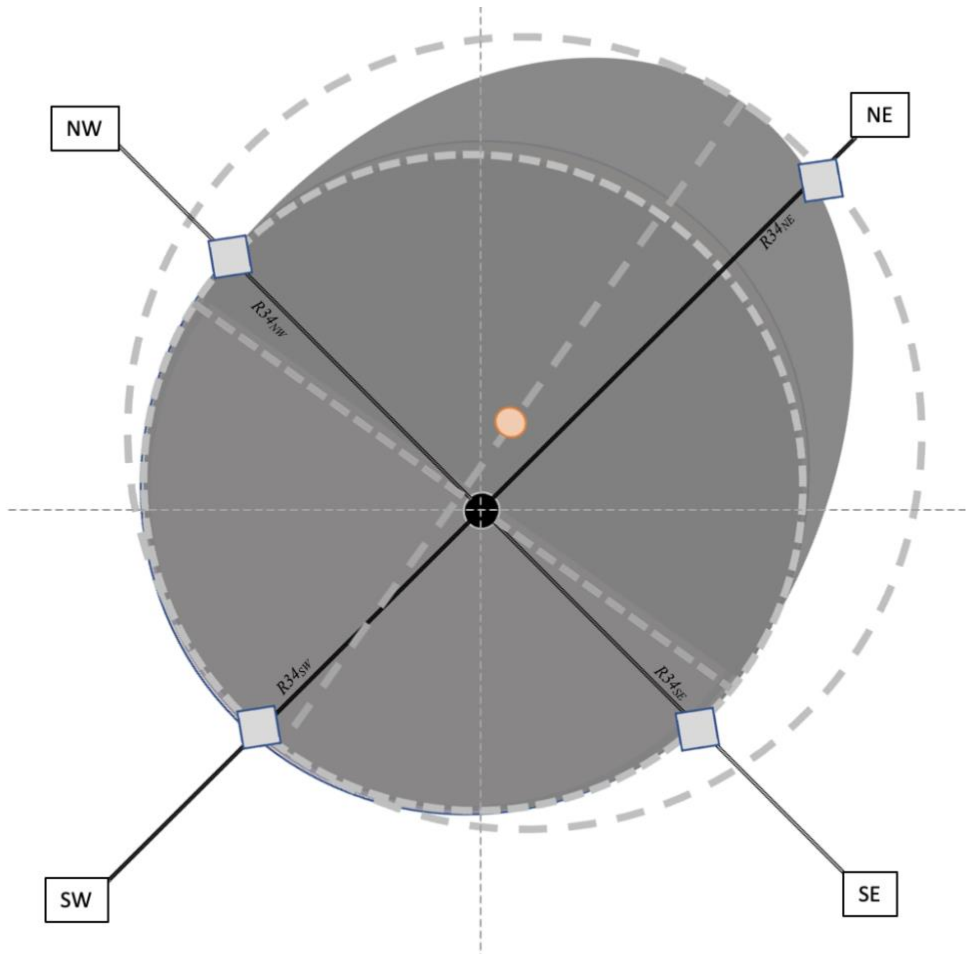

Figure 1. An example of estimated distribution area (gray shaded area) given 34-knot wind radii reported for each quadrant (gray diamonds) and a TC center location (black dot). Properties of the ellipsoid are defined by major and minor ellipse axes (gray dashed lines) and a displacement of the 34-knot wind distribution center (orange dot) from the TC circulation center, which indicates the relative rotation and shift of these center positions. Geometrically, this ellipsoid can be thought of as two imaginary circles whose radii define the major and minor axes and are shifted in space (gray dashed circles). In this example, $R34_{NE}$ defines the maximum extent of 34-knot winds in the system at this time, and $R34_{SW} < R34_{SE} < R34_{NW} < R34_{NE}$.

Goal(s): Improve the coverage of surface wind and wave observations to better quantify the distribution of hazards associated with a given tropical cyclone.

Hypotheses:

1. Aligning the flight pattern with the azimuth of expected surface wind distribution skew will better capture uncertainty in the direction of furthest extent of surface wind thresholds.

2. Obtaining better azimuthal coverage will aid in identifying deviations from symmetric mean wind and wave assumptions.
3. Azimuthally dense outer core surface wind observations can be used to compare the effect of inner core TC structure and nearby environment on the overall hazard characteristics exhibited by the targeted TC.

Objectives:

1. Sample region along azimuths of greatest outer core asymmetry to estimate uncertainty in the distribution of hazardous winds.
2. Identify differences between wind field distribution at flight level verses the surface by comparing wind values obtained by available onboard instrumentation in regions where uncertainty is expected to be greatest.
3. Improve azimuthal coverage of the inner and outer core by focusing on preferential azimuths expected to be affected by inner core and/or environmentally forced asymmetries.

Aircraft Pattern/Module Descriptions (see *Flight Pattern* document for more detailed information): This experiment requires modifications to typical P-3 patterns dependent on the approximated TC surface wind distribution. Estimates of the area, skew, and orientation of the surface wind distribution will be provided by the PIs during and prior to implementation of these patterns; these will dictate optimal azimuths and radial leg lengths. While it is expected that surface wind characteristics may not align perfectly with NHC-reported values, a first guess of the distribution will be calculated using the most recent wind radii provided by NHC for a given system. In-flight adjustments to the orientation and leg lengths may be required if observations reflect a substantially different surface wind distribution.

Adjustments to the legs of Figure-4 patterns aim to maximize azimuthal sampling of surface winds while maintaining necessary inner core coverage. Depending on available reconnaissance measurements and the estimated TC distribution size, different patterns may be more appropriate. The three patterns devised for this module were designed to cover various scenarios related to uncertainty in significant wind radii. Pattern 1 was designed to observe temporal variations in the quadrant of maximum extent, whereas Pattern 2 focuses on spatial variations in nearby quadrants at nearly the same time by reordering traditional legs of a Figure-4. Pattern 3 utilizes a combination of multiple wind radii estimates to better assess azimuthal variations in hazardous winds by prioritizing the region of largest extent. Regardless of pattern, multiple dropsondes may be necessary if inconsistencies exist between SFMR observations and the expected flight-level reduction estimates of surface wind. Additional dropsondes may be needed along downwind legs if the storm's size limits azimuthal coverage of observations; this is especially important in Pattern 1, or for storms with very large distribution coverage. The length of the legs in all patterns are defined by the smallest of either (a) R34 or (b) the radius of wind speed equal to 50% of the storm's intensity, which the PIs will provide to LPS.

Patterns 1 and 3 require an initial Figure-4 of the system with leg lengths scaled by quadrant size, and the initial azimuth can be adjusted to comply with other experiments/modules as long as the initial azimuth is within 20 degrees of the maximum radial extent. Pattern 2 reorders radial legs and can be performed in two ways, where an initial Figure-4 may precede the shown pattern when targeting distributions of higher wind speeds (inner core) or replaced by the pattern itself when focusing on the distribution of 34-knot winds (outer core). However, when possible, all patterns should be oriented to maximize the coverage of the distribution area. While radial leg lengths for all patterns will vary based on an asymmetric estimate of the wind distribution, Atlantic basin climatological estimates of symmetric averages for each significant wind radius is given in Table 1 (Kimball and Mulekar 2004) as a guide for flight duration.

Significant Radius	Minimum (n mi)	Maximum (n mi)	Median (n mi)
34-knot	25	375	110
50-knot	10	255	70
64-knot	10	125	45

Table 1. Climatological maximum, minimum, and median significant wind radii values given symmetric mean calculations from Best Track in the North Atlantic basin.

P-3 Pattern 1:
This is a modified version of a rotated figure-4 pattern where leg lengths may not be the same during all passes. Information on leg lengths and optimal azimuths will be provided by PIs and will require the LPS to communicate distribution characteristics observed during the first figure-4, primarily using available SFMR and dropsonde surface wind values.

Optimally, an initial figure-4 with leg lengths corresponding to the most recent NHC-reported wind radii quadrant information is oriented 20 degrees from ordinal direction axes (NE, SE, SW, NW), as directed by PIs. This can be adjusted to reach additional experiment objectives, but its inbound azimuth must align within 20 degrees of the estimated skew direction. When azimuthal orientation of the first Figure-4 does not align approximately in an ordinal direction due to other experiment priorities, the subsequent Figure-4 can be oriented directly on the ordinals or azimuth of anticipated maximum extent (see Figure 1). After the first figure-4 and a rotation of 40 degrees (preferred) or 45 degrees (acceptable), a second figure-4 is performed using characteristics observed during the first figure-4.

Dropsondes deployed near significant wind radii (R64, R50, R34) in coordination with remotely sensed observations along these axes aim to reduce the uncertainty in quadrant radii information; this may mean shifting midpoint dropsonde locations based on the surface wind extent, at the discretion of the LPS. Additional dropsondes may be requested in real-time to optimize azimuthal coverage per quadrant within the time window, including on downwind legs or where inconstancies exist between SFMR-reported surface winds and reduced flight-level wind estimates. The PIs will coordinate with LPS on potential locations where additional dropsondes may be needed and will require the LPS to watch for places when SFMR values equal or exceed flight-level reduction estimates outside of the RMW, especially outwards of twice the RMW.

P-3 Pattern 2:
This windmill pattern can be performed in two ways and intends to better estimate the azimuthal variation in wind radii in each quadrant by reordering radial legs within the 6-hour data assimilation time window. The ability to perform this pattern depends on the maneuverability within the center due to the turns between inbound and outbound legs. The storm should have a large enough eye to safely turn between legs in the center. Eye size and wind radii are not well correlated so both small and large TCs are of interest.

Here, the aircraft preferentially samples the regions defining areal skew axes of the wind distribution, which will be provided by the PIs. This strategy can reveal differences in wind distribution area and relative orientation between typical reduction level (700mb) and the surface. For very large TCs or when other priorities require a full Figure-4, this pattern should be scaled to 50- or 64- knot wind radii. The maximum wind in each quadrant will be used to determine radial dropsonde locations for each fan, where “mid-points” are defined as the significant wind radius (i.e., R50 or R64) closest to 75% of its quadrant’s maximum wind.

For smaller TCs (safety permitting) or for those not targeted by other experiments, this pattern begins with an initial transect oriented 20 degrees from the assessed wind distribution skew direction. Radial fans sample 40-degree pie slices per quadrant out to the radius of 34-knot winds. The maximum wind in each quadrant will be used to determine radial dropsonde locations for each fan, where “mid-points” are defined as the significant wind radius (i.e., R34, R50, or R64) closest to 50% of its quadrant’s maximum wind.

Additional dropsondes may be requested in real-time where inconsistencies exist between SFMR-reported surface winds and reduced flight-level wind estimates. The PIs will coordinate with LPS on potential locations where additional dropsondes may be needed and will require the LPS to watch for places when SFMR values equal or exceed flight-level reduction values outside of the RMW, especially outwards of twice the RMW.

P-3 Pattern 3:
This pattern takes advantage of multiple significant wind radii to preferentially sample regions that need better azimuthal coverage given the wind distribution, where leg lengths and azimuths will be provided by the PIs using NHC-reported wind radii values. The storm should have a large enough eye to safely turn between spokes in the center. Eye size and wind radii are not well correlated so both small and large TCs are of interest.

Similar to previous patterns, an initial figure-4 with quadrant-dependent leg lengths is performed, followed by a downwind leg 40 degrees counter-clockwise and inbound leg. As opposed to Pattern 1, the orientation of this Figure-4 must lie within 40 degrees of gale-force wind distribution skew axes.

Following the first figure-4, the downwind turn can be omitted if the wind distribution skews among 34-, 50-, and/or 64-knot wind radii are similar in orientation, or if the azimuthal differences are within 30 degrees of the initial Figure-4 azimuths. In this situation, the aircraft turns around and heads inbound on the same azimuth. This information will be provided by the PIs in real time before choosing an inbound leg.

Once in the center after the inbound leg, instead of continuing along the azimuth, turn outward along inner radii distribution skew direction (as in Pattern 2 but for radius of 50-knot winds for most TCs; radius of 64-knot wind used for TC intensities greater than 130 knots) to begin the first spoke. Once surface wind speeds decrease by half from quadrant maximum, or when is safe, the P-3 should turn around and head inbound on the same azimuth. The following 2-3 additional spokes sample the quadrant counterclockwise of calculated skew direction every 30-45 degrees depending on the size of the storm. It is important to note that distribution skew for each significant wind radius often displays different shapes and orientations at a given time. It is therefore crucial for this pattern to rely on multiple wind distribution representations for the initial Figure-4 (overall hazardous wind field) and for the spokes (the wind field at the boundary between inner and outer core); this will be a coordination between the PIs and the LPS in real-time.

Dropsondes will be deployed at typical end- and mid-points during the Figure-4, and at the endpoints and mid-points of each spoke. Additional spokes can be performed if time permits, continuing counterclockwise around the system, where spoke leg lengths are dependent on its respective quadrant's wind radii. Alternatively, previous spoke azimuths can be repeated if necessary to verify collected measurements so long as the quadrant counterclockwise of the calculated skew distribution is azimuthally well observed.

Additional dropsondes may be requested in real-time where inconstancies exist between SFMR-reported surface winds and reduced flight-level wind estimates. The PIs will coordinate with LPS on potential locations where additional dropsondes may be needed and will require the LPS to watch for places when SFMR values equal or exceed flight-level reduction values outside of the RMW, especially outwards of twice the RMW**.**

Links to Other Mature Stage Experiments/Modules: It is preferred to link other experiments to the goals outlined here when possible. This experiment can be performed in conjunction with many other Early/Mature/End stage experiments and can be modified to supplement the wind coverage obtained for other experiment objectives. Optimal wind observation coverage includes regularly operated instruments (SFMR, TDR, GPS dropsondes) and supplemental research instrumentation (IWRAP, WSRA, KaIA, CRL, etc.) to ensure the best representation of surface winds.

Other experiments and modules may provide significant benefit to this coverage strategy especially when additional aircraft (P-3, G-IV, UAS) and instrumentation can be leveraged to observe complementary parts of the storm, as in ITOFS or RICO SUAVE. When the TC is very large, complimentary G-IV circumnavigation coverage can aid in the observation of outer core winds.

Other Mature Stage experiments and modules such as Surface Wind and Wave Validation, Gravity Wave, Hurricane Boundary Layer, NESDIS Ocean Winds, TC Diurnal Cycle, TDR Analysis Evaluation and Ocean Survey/Sustained Targeted Ocean strategies can provide significant benefit when investigating causes for asymmetry. Moreover, objectives from Early (AIPEX) and End Stage (TC at Landfall and Extratropical Transition) experiments directly address asymmetries related to environmental factors (VWS, ET) and landfalling forecast uncertainty.

The orientation of Patterns 1, 2, and 3 can be adjusted to account for priorities in other experiments but must reasonably estimate the extent of hazardous winds in each quadrant. Pattern 2 may fulfill requirements for other experiments despite the rearranging of radial legs in time, but it does require an azimuthal orientation approximately along the estimated distribution skew axis.

Analysis Strategy: All patterns require real-time estimates of wind radii by quadrant, including NHC-reported significant wind radii and airborne measurements. Estimates of surface wind distribution skew will be provided by the PIs and are based on asymmetric ellipses whose axes are defined by available significant wind radii values (Figure 1). While data coverage may differ from conventional operational locations, all dropsonde information will be transmitted during flight to be included in real-time HAFS analyses. This will be important for identifying biases in boundary layer structure within the HAFS framework (Poterjoy 2022).

Each pattern addresses specific questions related to wind distributions in TCs, and all patterns aim to provide observations that may aid in reducing uncertainty in hazardous surface wind estimates. This directly impacts wave and surge models that rely on accurate surface winds as their input. Therefore, the analysis strategy regardless of specific patterns flown will include asymmetric quantifications of hazardous winds by increasing the azimuthal coverage in the outer core. This allows for a comparison between geometric area and traditional polar wavenumber analyses which may expose atmospheric mechanisms responsible for its asymmetry.

Pattern 1 directly addresses questions related to significant wind radii errors and uncertainty, comparing multiple radials within the same quadrant to inspect the reported significant radii information. This may also expose outer core wind hazard variability between passes. Patterns 1 and 2, while similar in coverage, address uncertainty in different ways. Where Pattern 1 investigates the uncertainty in overall wind field area within a time window, Pattern 2 focuses on variations in each quadrant at their respective measurement times. Pattern 3 focuses on the quadrant with the largest outer core extent as defined by the significant radius closest to 50% of the observed intensity. This pattern's coverage should be able to reflect radial and azimuthal variations in surface winds within the outer and inner core by beginning with a full coverage of the distribution area and inspecting the region between the inner core and the environment that covers the largest geographical area. In addition, anytime reduction values calculated using flight level (700 mb or 850 mb) exceed the expected symmetric mean ratio (0.9 at 700 mb or 0.8 at 850 mb for the eyewall; 0.85 at 700 mb or .0.8 at 850 mb for outer vortex in convection; 0.8 at 700 mb or 0.75 at 850 mb for outer vortex not in convection; Franklin et al. 2003), additional dropsondes must be deployed to directly measure the vertical structure of winds to the surface.

Data collected will be used to quantify uncertainty in surface wind distribution by quadrant as it relates to TC-related processes on all scales of motion. During and after each flight, available surface wind measurements will be compared to NHC-reported wind radii in each quadrant and compared to the initial estimate of the distribution area. While uncertainty in center location may strongly affect the location of highest winds, this area estimate is less sensitive to uncertainty in center location since it relies on the relative position of the outer bounds of the significant wind radii. This 2-dimensional distribution estimate can be applied to any vertical level and can thus be used to compare asymmetric structure between 700 mb or 850 mb and the surface. If reduction assumptions collapse, the additionally aforementioned dropsondes will be used to analyze differences between observed surface winds and winds calculated using axisymmetric reduction assumptions. These observations will help to validate and adjust existing strategies related to the quantification of surface distribution shape (ellipsoid or other) which can be used to analyze large model datasets, including operational global and regional weather prediction models as well as climate and ocean models focusing on TC impacts.

References:

Bowyer, P. J., and A. W. MacAfee, 2005: The Theory of Trapped-Fetch Waves with Tropical Cyclones—An Operational Perspective. *Wea. Forecasting*, 20, 229–244, https://doi.org/10.1175/WAF849.1.

Callaghan, David P., J. Callaghan, P. Nielsen, and T. Baldock, 2007: Generation of Extreme Wave Conditions from an Accelerating Tropical Cyclone. Coastal Engineering., 752-760, https://doi.org/10.1142/9789812709554_0064.

Chavas, D. R., N. Lin, W. Dong, and Y. Lin, 2016: Observed Tropical Cyclone Size Revisited. *J. Climate*, 29, 2923–2939, https://doi.org/10.1175/JCLI-D-15-0731.1.

Collins, C. O., H. Potter, B. Lund., H. Tamura, & H. C. Graber, 2018: Directional wave spectra observed during intense tropical cyclones. *Journal of Geophysical Research: Oceans*, 123, 773– 793. https://doi.org/10.1002/2017JC012943.

Esquivel-Trava, B., F. J. Ocampo-Torres, & P. Osuna, 2015: Spatial structure of directional wave spectra in hurricanes. *Ocean Dynamics*, 65, 65– 76.

Franklin, J. L., M. L. Black, and K. Valde, 2003: GPS dropwindsonde wind profiles in hurricanes and their operational implications. Wea. Forecasting, 18, 32–44, doi:10.1175/1520-0434(2003)018<0032:GDWPIH>2.0.CO;2.

Franklin, J., Black, M, and Valde, K. 2000: Eyewall Wind Profiles in Hurricanes Determined By GPS Dropwindsondes. National Hurricane Center., https://www.nhc.noaa.gov/aboutwindprofile.shtml#fig1

Houghton, I. A., C. Hegermiller, C. Teicheira, & P. B. Smit, 2022: Operational assimilation of spectral wave data from the Sofar Spotter network. *Geophysical Research Letters*, 49, e2022GL098973. https://doi.org/10.1029/2022GL098973

Hu, K., & Chen, Q., 2011: Directional spectra of hurricane-generated waves in the Gulf of Mexico. *Geophysical Research Letters*, 38, L19608. https://doi.org/10.1029/2011GL049145

Kimball, S. K., and M. S. Mulekar, 2004: A 15-Year Climatology of North Atlantic Tropical Cyclones. Part I: Size Parameters. *J. Climate*, 17, 3555–3575, https://doi.org/10.1175/1520-0442(2004)017<3555:AYCONA>2.0.CO;2.

Knaff, J. A., S. P. Longmore, and D. A. Molenar, 2014: An Objective Satellite-Based Tropical Cyclone Size Climatology. *J. Climate*, 27, 455–476, https://doi.org/10.1175/JCLI-D-13-00096.1.

Landsea, C. W. and J. L. Franklin, 2013: Atlantic Hurricane Database Uncertainty and Presentation of a New Database Format. Mon. Wea. Rev., 141, 3576-3592.

MacAfee, A. W., and P. J. Bowyer, 2005: The Modeling of Trapped-Fetch Waves with Tropical Cyclones—A Desktop Operational Model. *Wea. Forecasting*, 20, 245–263, https://doi.org/10.1175/WAF850.1.

Reasor, P. D., M. T. Montgomery, F. D. Marks Jr., and J. F. Gamache, 2000: Low-wavenumber structure and evolution of the hurricane inner core observed by airborne dual-doppler radar. *Mon. Wea. Rev.*, 128, 1653–1680, doi:10.1175/1520-0493(2000)128<1653:LWSAEO>2.0.CO;2.

Poterjoy, J., 2022: Implications of Multivariate Non-Gaussian Data Assimilation for Multiscale Weather Prediction. *Mon. Wea. Rev.*, 150, 1475–1493, https://doi.org/10.1175/MWR-D-21-0228.1.

Powell, M. D. and P. G. Black, 1990: The relationship of hurricane reconnaissance flight-level wind measurements to winds measured by NOAA's oceanic platforms. *J. Wind Engineering and Industrial Aerodynamics*, 36, 381-392.

P.B. Smit, I.A. Houghton, K. Jordanova, T. Portwood, E. Shapiro, D. Clark, M. Sosa, T.T. Janssen, 2021: Assimilation of significant wave height from distributed ocean wave sensors. Ocean Modelling, 159 (2021), Article 101738.

Shao, Z., B. Liang, W. Sun, R. Mao, D. Lee, 2023: Whitecapping term analysis of extreme wind wave modelling considering spectral characteristics and water depth. Continental Shelf Research, Volume 254, 104909, 0278-4343, https://doi.org/10.1016/j.csr.2022.104909.

Uhlhorn, E. W., B. W. Klotz, T. Vukicevic, P. D. Reasor, and R. F. Rogers, 2014: Observed Hurricane Wind Speed Asymmetries and Relationships to Motion and Environmental Shear. *Mon. Wea. Rev.*, 142, 1290–1311, https://doi.org/10.1175/MWR-D-13-00249.1.

Wright, C. W., E. J. Walsh, D. Vandemark, W. B. Krabill, A. W. Garcia, S. H. Houston, M. D. Powell, P. G. Black, and F. D. Marks, 2001: Hurricane directional wave spectrum spatial variation in the open ocean. J. Phys. Oceanogr., 31, 2472–2488.

Young, I. R. (2006). Directional spectra of hurricane wind waves. *Journal of Geophysical Research*, 111, C08020. https://doi.org/10.1029/2006JC003540

Young, I. R. 2017. "A Review of Parametric Descriptions of Tropical Cyclone Wind-Wave Generation" *Atmosphere* 8, no. 10: 194. https://doi.org/10.3390/atmos8100194

Zhang, J. A., R. F. Rogers, D. S. Nolan, and F. D. Marks, 2011: On the Characteristic Height Scales of the Hurricane Boundary Layer. *Mon. Wea. Rev.*, 139, 2523–2535, https://doi.org/10.1175/MWR-D-10-05017.1.